A New Laparoscopic Tool With In-Hand Rolling Capabilities for Needle Reorientation

Giuseppe Andrea Fontanelli, *Student Member, IEEE*, Mario Selvaggio, *Student Member, IEEE*, Luca Rosario Buonocore, Fanny Ficuciello, *Senior Member, IEEE*, Luigi Villani, *Senior Member, IEEE*, and Bruno Siciliano, *Fellow, IEEE*

***Abstract*—In laparoscopic minimally invasive robotic surgery, a teleoperated robot is interposed between the patient and the surgeon. Despite the robot aid, the manipulation capabilities of surgical instruments are far from those of the human hand. In this letter, we want to make a step forward toward robotic solutions that can improve manipulation capabilities of the surgical instruments. A new concept of needle-driver tool is presented, which takes inspiration from the human hand model. The idea is to modify a standard laparoscopic tool by introducing an additional degree of freedom, which allows in-hand reorientation of the suturing needle. A 3D printed prototype has been built to validate the tool design. The improved manipulation capabilities have been assessed quantitatively by evaluating a weighted dexterity index along a single stitch trajectory. Moreover, a comparison between our tool and a standard needle driver has been done in terms of time required for the execution of a complete suturing sequence.**

***Index Terms*—Surgical robotics, laparoscopy, mechanism design, grippers and other end-effectors, dexterous manipulation, contact modeling.**

I. Introduction

SOME of the most critical and delicate tasks in laparoscopic Minimally Invasive Robotic Surgery (MIRS) are reconstructive procedures because of their time demand, the high dexterity required, the risks of causing damage to organs and/or tissues and the risks related to poorly executed sutures. These procedures are very difficult and stressful even for a skilled surgeon, mostly because of the reduced workspace, the high precision required, the lack of haptic perception and the complexity induced by artificial vision feedback.

Common robotic surgical instruments used in MIRS are designed to extend the surgeon dexterity in such delicate procedures. For instance, the da Vinci Surgical System is ideally suited for this scope, thanks to the EndoWrist technology from Intuitive Surgical, that allows articulated motion of the surgical tool and tremor filtering.[1] The EndoWrist system mimics the human wrist capabilities adding two extra degree-of-freedom (DoF) to the standard laparoscopic instruments, which are mostly rigid and straight tools ending with a gripper. In this way, the surgeon dexterity is comparable to that achieved in open surgery using a standard needle-holder forceps.

More advanced suturing tools have been developed for laparoscopic interventions to allow automatic suturing executions; this is the case of the Endo360[2] and the PROXISURE.[3] These smart instruments are not yet available for the da Vinci robot and do not give the surgeons the total control of the needle motion neither allow to select the best needle type and pose for each surgical procedure. Despite the development of enhanced laparoscopic tools [1], surgeons' manipulation capabilities are still far from those of the human hand.

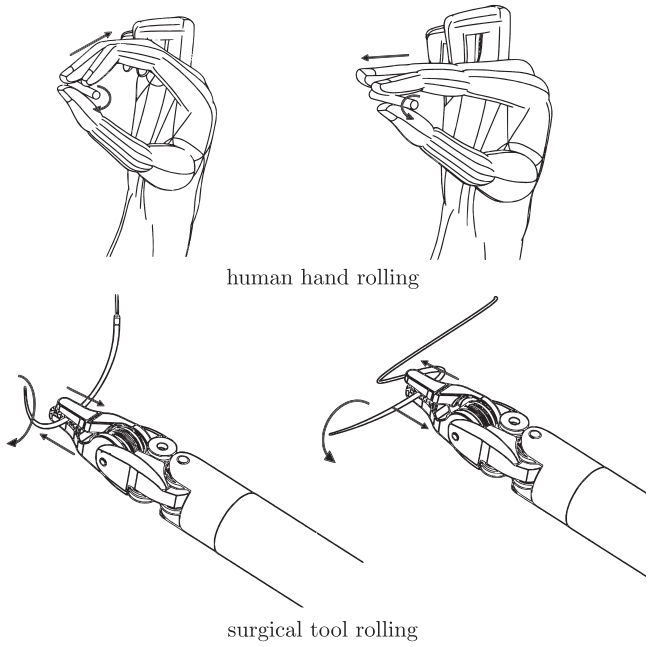

Fig. 1. Object rolling capability of the novel suturing tool inspired by that of the human hand.

Manuscript received September 10, 2017; accepted January 28, 2018. Date of publication February 27, 2018; date of current version March 28, 2018. This letter was recommended for publication by Associate Editor I. I. Iordachita and Editor K. Masamune upon evaluation of the reviewers' comments. This work was supported in part by the EC Seventh Framework Programme (FP7) within RoDyMan Project 320992 and in part by the STAR 2016 Programme within MUSHA Project. *(Corresponding author: Mario Selvaggio.)*

The authors are with the Interdepartmental Center for Advances in Robotic Surgery, University of Naples Federico II, Naples 80125, Italy (e-mail: g.a.fontanelli@gmail.com; mar.selvaggio@gmail.com; lucarosario.buonocore@unina.it; fanny.ficuciello@unina.it; lvillani@unina.it; siciliano@ieee.org).

Digital Object Identifier 10.1109/LRA.2018.2809443

[1]http://www.davincisurgery.com/da-vinci-gynecology/ da-vinci-surgery/da-vinci-surgical-system/system-sa- fety.php

[2]http://www.endoevolution.com/endo360

[3]http://www.ethicon.com/healthcare-professionals/ products/advanced-suturing-system/proxisure-suturing-devices

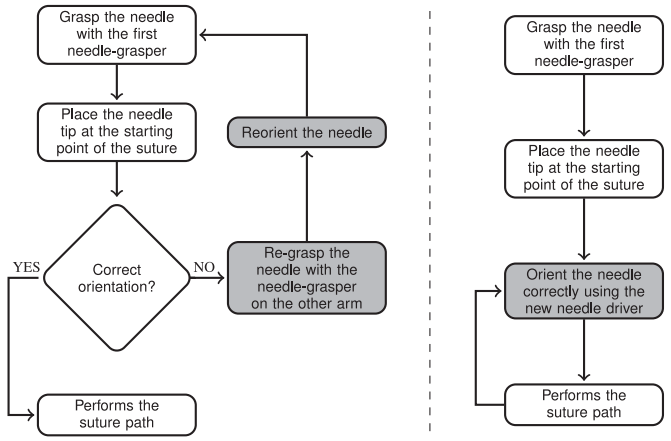

Fig. 2. Suturing sequence flow charts. Left: standard tool (ST); right: modified tool (MT). The steps involving needle reorientation are highlighted in gray.

During suturing, the surgeon needs to constantly change the orientation of the needle in order to find the appropriate pose. To this end, the reorientation phase is conducted through successive grasp and release operations, according to a *grasping - release - positioning - re-grasping* sequence, using both arms of the robot. This sequence of operations is shown in the flow chart on the left of Fig. 2.

This problem may be overcome by modifying the needle driver with a slot specifically designed to keep the needle perpendicular to the gripper [2], [3]. However, even in this case, the needle position and orientation inside the gripper would not be under the surgeon's control.

In some cases, also the reaching of instrument's joint limits might require releasing and re-grasping the needle in a different configuration with the second arm intervention. Haptic cues have been be employed to inform the operator about joint limits [4], [5] but dual arm reorientation cannot be avoided.

Starting from these premises, we believe that an additional DoF can be extremely useful to manipulate rigid objects with a circular cross section, such as, needles for suturing. In this work, a new needle driver tool that allows a more natural and intuitive manipulation of the surgical needle is presented. Inspired by the human hand motion (see Fig. 1), our design enables the possibility to reorient the suturing needle without interruptions, controlling the additional DoF of the tool in telemanipulation or in autonomous mode. Hence, some surgical tasks, such as suturing, might be executed using only one arm. To the best of our knowledge, there are no surgical tools specifically designed for in-hand manipulation.

The rest of this letter is organized as follows: Section II presents the motivation of the work and clinical needs; in Section III the novel tool design solution is detailed; Section IV presents a scale prototype of the tool used to test the mechanical design; Section V discusses the results obtained in two case studies while Section VI concludes the letter. Finally, the Appendix presents the weighted dexterity index used to compare the manipulation capability of the proposed instrument with that of a standard da Vinci instrument.

II. Motivation

Our work takes inspiration from the study presented in [6] in which the most common surgeons movements performed during open surgery are evaluated. Among these movements, two are of interest for the purpose of the presented work: *"rolling between fingers"* and *"rolling for reorientation"*. These two movements are common both during tissue and needle manipulation and are not performable using the currently adopted robotic surgical instruments. On the other hand, several works can be found in the recent robotic literature focusing about the development of advanced grippers for in-hand manipulation. For instance, in [7]–[9] three different designs concepts are presented. Our approach aims at transferring the most recent results in robotic manipulation to the robotic surgical scenario.

In this work, we focus in particular on the suturing procedure, defined as a row of stitches holding together the edges of a wound or surgical incision. Suturing is one of the most challenging tasks in minimally invasive surgery and micro surgery [10], [11]; an error in suturing can produce significant tissue damage and is more likely to happen when the needle orientation is not completely under the surgeons control [3], especially in absence of force feedback information [12]–[14]. Due to the structure of standard needle drivers, the orientation of the needle during the suturing procedure is not completely controllable and multiple pairs of hand-off movements are required, before the execution of each stitch [3].

An evaluation of the occurrence of this behavior can be found by inspecting replicated suturing procedures. To this end, we have considered the suturing video data in the JHU-ISI Gesture and Skill Assessment Working Set (JIGSAWS) [15], captured using the da Vinci Research Kit [16]. The database comprises 39 suturing tasks each composed of four stitches on a bench-top model, performed by eight surgeons with different levels of skills. In addition to this, we have also inspected a number of videos acquired during in vivo surgical procedures performed by expert surgeons. In the considered videos, we counted the number of stitches that require needle reorientation and measured the average and the variance of time lost in this operation, for the three levels of surgical skills. The results in Fig. 3 show that the percentage of stitches requiring needle reorientation is rather high, although it decreases when the surgeons' skills increase. The same trend can be observed for the average time lost. It is worth noting that in the real scenarios, in which the needle needs to be dropped and re-grasped to make knots or move organs, the number of stitches requiring reorientation is considerably higher than for the sutures performed on the bench-top model.

III. Working Principle

In this section, the working principle of the new suturing tool is described.

A. Mechanics

In this work, a gripping mechanism capable of impressing tangential motions to a circular cross section object has been

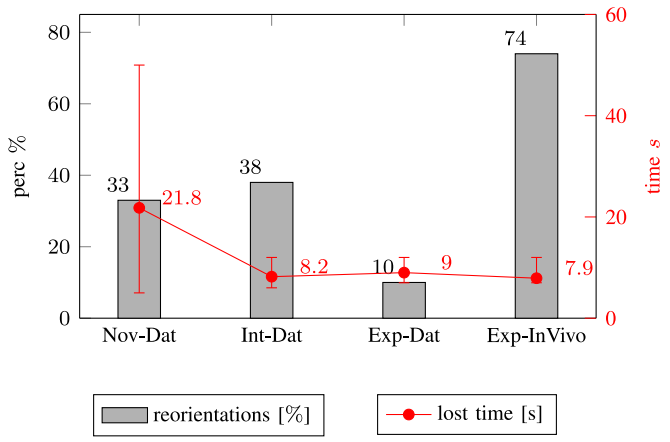

Fig. 3. Percentage of stitches requiring needle reorientation and average/variance of the time lost for reorienting the needle. Data provided by the JIGSAWS dataset (-Dat) and real procedures (-InVivo) performed by novice (Nov-), intermediate (Int-) and expert (Exp-) surgeons.

designed and developed. The tendon driven actuation mechanism of a standard da Vinci laparoscopic tool has been modified by adding an additional pulley used to actuate the extra DoF responsible for the rolling motion. This solution is fully compatible with the instruments of the ultimate da Vinci robots, such as the da Vinci Xi, which is equipped with an extra actuated DoF that can be used for advanced tools.

The design of the tool has been carried out considering the following constraints:

- the external radius of the tool must be smaller than the internal radius of the trocar (8.5 mm) used by the da Vinci robotic system;
- the dimensions of the two fingers must be equal to those of the fingers of the da Vinci standard needle driver tool whose efficiency has been largely demonstrated in their long time of use.

Moreover, the maximization of the rolling motion that can be impressed to the most used needles in laparoscopic procedures [17] has been taken in to account.

Fig. 4 shows an exploded view of the conceived tool. The fingers 6A and 6B are actuated indirectly by the pulleys 7A and 7B to allow the fingers rotation. The pulley 8 creates the desired linear displacement along the fingers major direction. To this end, the pulley 8 has been designed with two eccentric cylinders disposed specularly with a phase displacement of 180° (8-1 in Fig. 4). These cylinders rotate within two slots made on the fingers to produce a linear motion. Two linear guides, represented by the parts 7A-1 and 6A-1 in Fig. 4, are used to constrain the linear motion between the fingers and the pulleys 7A and 7B. Therefore, a rotation of the eccentric cam causes a shift of the finger with respect to its rest position. Conversely, leaving the cam in the rest position (see Fig. 5 on the center) the fingers remain aligned. The actuation of the pulleys 7A, 7B and 8 is obtained by means of three pairs of tendons (direct and antagonist) fixed to the respective pulleys.

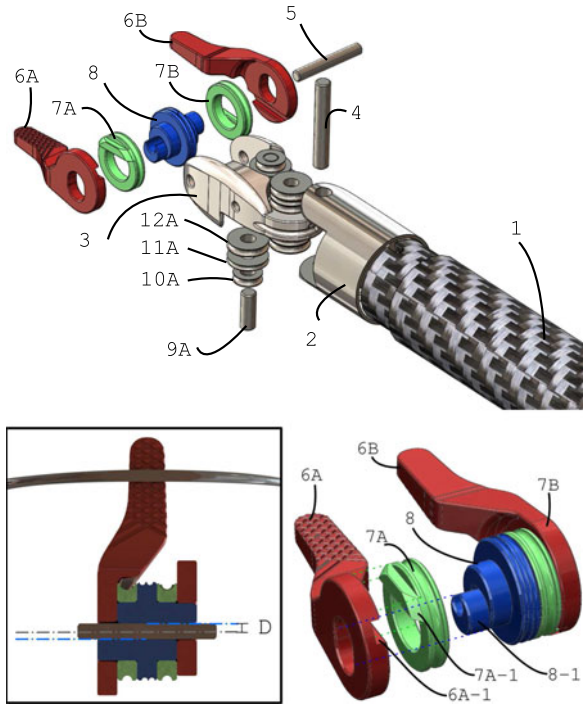

Fig. 4. The new suturing tool: Exploded view and cross section (in the frame).

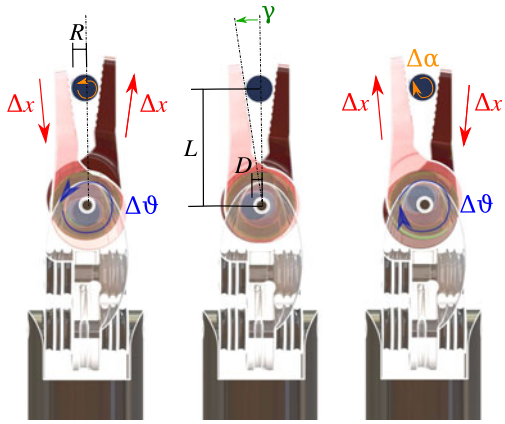

Fig. 5. New suturing tool working principle. A rotation of the internal pulley of an angle $\Delta\vartheta$ causes the opposite translation of the two fingers (Δx) and hence the rotation of the grasped object of an angle $\Delta\alpha$.

B. Mathematical Model

The displacement Δx of the two fingers is mechanically related to the central pulley rotation angle $\Delta\vartheta$ (see Fig. 5). This displacement causes a certain rotation $\Delta\alpha$ of the cylindrical object depending on the object radius and on its position between the fingers. Assuming no slippage between the object and the fingers, the following equations hold

$$\begin{cases} \Delta x = D\,\sin(\Delta\vartheta) \\ \Delta x = R\,\Delta\alpha \end{cases} \implies \Delta\alpha = \frac{D\,\sin(\Delta\vartheta)}{R} \qquad (1)$$

where R is the object radius and D is the misalignment between the center of the central pulley and the center of the eccentric (refer to Fig. 4).

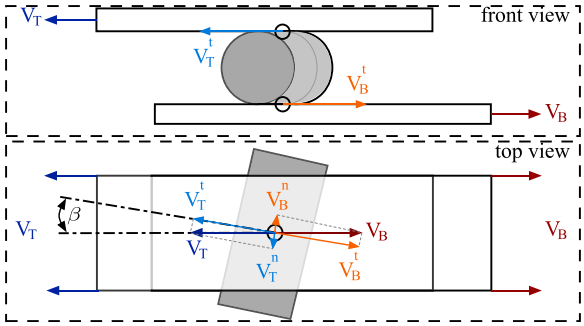

Fig. 6. Rolling model representation.

To maximize the rolling capability of the tool, the needle needs to be grasped with its tangent parallel to the tool joint axis (the axis of the pulley 8 in Fig. 4). If there is a misalignment the velocity impressed by the instrument is not converted only into a rolling velocity but another component is determined.

In Fig. 6 this behavior is shown more in details: consider two planes that translate in two opposite directions with velocities V_T and V_B and a cylinder in contact with the two planes oriented with an angle β with respect to the direction of motion. The velocity V_B can be decomposed into two components V_B^t, V_B^n, where

$$V_B^t = V_B \cos(\beta) \qquad V_B^n = V_B \sin(\beta) \tag{2}$$

and the same equations can be written for the V_T velocity. Then, (1) must be rewritten taking into account that the rolling motion when $\beta \neq 0$ is reduced by $\cos(\beta)$

$$\Delta\alpha = \frac{D \sin(\Delta\vartheta)}{R} \cos(\beta). \tag{3}$$

Therefore, if the angle β is not equal to zero, both the normal and tangential components of the velocities V_B and V_T are different from zero. Notice that the normal velocities V_B^n and V_T^n are realizable only considering slippage in the direction of the object axis. Hence, if $\beta \neq 0$, during the rolling motion a higher velocity is required to rotate the needle by the same quantity, resulting in a more expensive operation. This means that, if the needle is not gripped with its tangent orthogonal to the direction of motion of the two fingers, the needle can be still rotated but a lower angular displacement can be accomplished.

To comply with specifications of Section III-A, a constraint on the misalignment D has been imposed. In particular, we choose $D = 0.5$ mm while $\Delta\vartheta$ is in the range $[-\pi/2, \pi/2]$. The rolling angle ranges for four classes of needle, most used in laparoscopic surgery, with three different β values can be computed using (3) are given in Table I.

Finally, the aperture angle of the gripper γ is related to the object radius and to the distance of the object from the gripper center of rotation (R and L in Fig. 5) by the equation

$$R = L \sin(\gamma) \quad \Longrightarrow \quad \gamma = \arcsin\left(\frac{R}{L}\right). \tag{4}$$

TABLE I
MAXIMUM ROLLING ANGLES FOR DIFFERENT NEEDLES

	R [mm]	$\beta = 0$	$\beta = \pi/12$	$\beta = \pi/4$
RB-1	0.25	$\pm 114°$	$\pm 110.1°$	$\pm 80.3°$
SH-Plus	0.352	$\pm 88°$	$\pm 85°$	$\pm 62°$
GL-222	0.38	$\pm 81°$	$\pm 78.2°$	$\pm 57°$
UR-6	0.5	$\pm 57.5°$	$\pm 55.3°$	$\pm 40.5°$

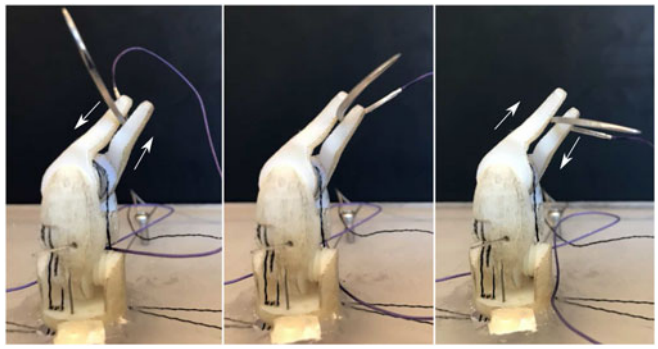

Fig. 7. 3D printed prototype of the new tool (scale 2:1): Evaluation of the working principle with a circular shape needle.

IV. SCALE PROTOTYPE

Due to the difficulty of having a complete and fully functional metal tool attached to a surgical robot, the evaluation of the mechanism has been carried out through a plastic 2:1 scale prototype.

The prototype was realized using a 3D printed technology based on the polyjet process.[4] This technology allows achieving sufficiently high precision and accuracy.

Fig. 7 shows a sequence of the motion. The mechanism was manually actuated by tendons and the executed rotation angle was measured using a protractor. The experiments were performed on a needle with a circular cross-section with diameter doubled with respect to the SH-Plus needle. When the tendons were actuated to move the mechanism in the entire range of motion, we measured an angle of about 80°. This value is close to the predicted value of 88° for a SH-plus needle actuated using a non-scaled tool. Hence, despite the high friction of the employed material and the errors introduced by a non perfect needle alignment, the experiments showed a working behaviour of the prototype close to the expected one.

V. CASE STUDIES

To measure the performance of the new needle driver we considered a set of real suturing procedures executed on da Vinci Research Kit (DVRK) with a standard tool (ST) and replicated them in a simulated environment with our modified tool (MT). Two case studies have been considered: the first is focusing on a *single stitch* trajectory execution; in the second, *complete sutures* procedures are considered, all with 5 stitches performed on different phantoms.

[4]http://www.stratasys.com/3d-printers/design-series/objet24

TABLE II
DH PARAMETERS OF THE MODIFIED TOOL (MT)

Link	Joint	Prev	Succ	a_i [m]	α_i [rad]	d_i [m]	θ_i [rad]
1	R	–	2	0	$\pi/2$	–	θ_4
2	R	1	3	0.009	$-\pi/2$	–	$\theta_5 + \pi/2$
3	R	2	4	L	0	–	θ_6
4	R	3	–	0	$-\pi/2$	–	$\theta_7 - \pi/2$

The goal of the analysis is to prove that our MT can both improve the surgeon precision and reduce the execution time by allowing in-hand needle reorientation during real suturing procedures. Moreover, we show that our tool is able to overcome the problem of reaching joint limits, within the range of movement.

Given these good results obtained on the scale prototype, in our simulation we have assumed that the MT is able to rotate the needle as expected, without slipping.

A. Simulation Environment

The simulation environment is composed by a simulated Patient Side Manipulator (PSM) of the da Vinci Research Kit that can be equipped with ST and MT. The simulator has been developed in V-REP and interfaced with the Master Tool Manipulator (MTM) of the da Vinci robot. Simulated trajectories have been planned with MATLAB.

PSM Arm: The PSM arm is a 7-DoFs actuated arm, which moves the attached instrument around a Remote Center of Motion (RCM), i.e., a mechanically-fixed point that is invariant with respect to the configuration of the PSM joints. In detail, the first 3 DoFs correspond to Revolute (R) and Prismatic (P) joints, in a RRP sequence and allows the rotation and translation of the surgical tools around the RCM. Moreover, the last 3 DoFs, in a RRR sequence, constitute the instrument wrist. Finally, the last degree of freedom (seventh) allows opening/closing of the grippers jaw. For more details on the robot kinematics the reader can refer to [18].

Tools: Two different tools carried by the first 3 PSM DoFs are used in the case studies: the first is the ST whose kinematic model is that described in [18]; the second is our MT whose kinematic is described by the DH parameters in Table II. In detail, the MT is a 4-DoFs kinematic chain in which the first 3-DoFs are the three joints of the ST wrist. The fourth DoF corresponds to a joint placed in the center of the circular section of the needle at the grasping point and is used to model the rotation induced by our mechanism. Notice that, in the experiments, we will assume that the object is already grasped and then the opening/closing DoF is not explicitly taken into account.

B. First Case Study: Single Stitch

Due to its kinematic structure, the PSM arm of the DVRK can easily reach configurations that are near to joint limits. When this happens, the real trajectory of the robot PSM may deviate from the trajectory commanded by the surgeon through the master robot, because of the occurrence of joint saturations.

TABLE III
ROBOT JOINT LIMITS (IN METERS OR RADIANS)

	q_1 [rad]	q_2 [rad]	q_3 [m]	q_4 [rad]	q_5 [rad]	q_6 [rad]	q_7 [rad]
Std.	$\pm\pi/2$	$\pm\pi/3$	[0, 1]	$\pm 3/2\pi$	± 1.39	± 1.39	–
Mod.	$\pm\pi/2$	$\pm\pi/3$	[0, 1]	$\pm 3/2\pi$	± 1.39	± 1.39	± 1.4

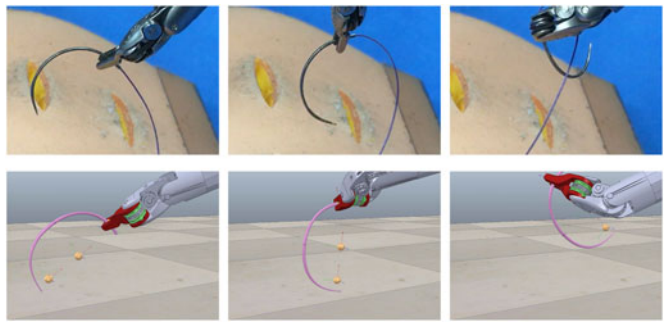

Fig. 8. Snapshots sequence of a single stitch trajectory. Top: standard tool (ST); Bottom: modified tool (MT).

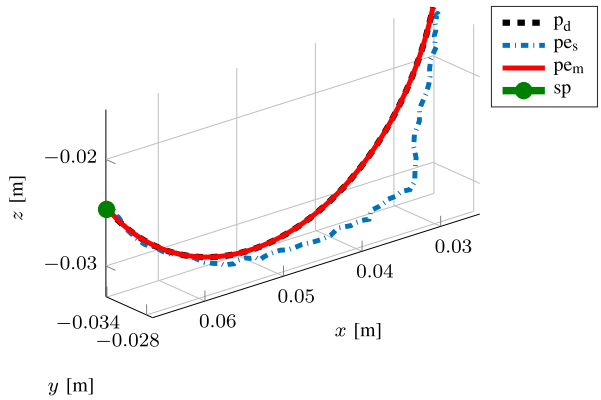

Fig. 9. Needle tip paths. pe_s is the path performed using the ST, p_d is the desired circular path and pe_m is the path simulated using the MT. The point sp is the trajectory starting point.

The goal of this case study is that of showing how our instrument could help to overcome this problem. To this end, an experiment was carried out using the ST mounted on the PSM arm: a needle trajectory along a circular path was commanded through the master robot, starting from a configuration close to a joint limit, so that joint saturations occur. Then, the desired circular trajectory was extrapolated using the part of the real trajectory not influenced by joint saturations. This desired trajectory was used in simulation as reference for the model of the PSM arm with the MT.

The joint limits considered in the experiments are given in Table III. A standard inverse kinematics algorithm has been implemented to solve for the da Vinci PSM joint values given the desired position and orientation of the needle frame [19]. Fig. 8 contains some snapshots from the real performed trajectory and the V-REP simulated environment.

The different behaviour of the two instruments can be better understood by looking at Fig. 9 showing the needle tip path executed using the ST (pe_s) and our MT (pe_m), respectively.

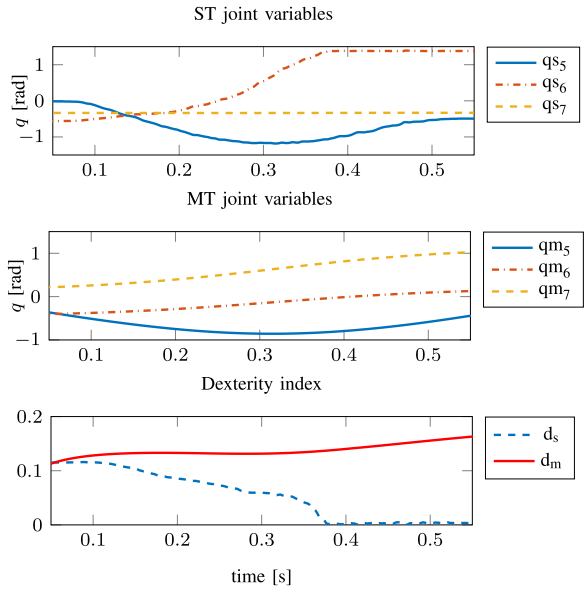

Fig. 10. Numerical results for the single stitch trajectory. Top: time history of the joint variables for ST; Middle: time history of the joint variables for MT. Bottom: time history of the dexterity index with ST (d_s) and MT (d_m).

When the ST is used, due to the presence of the joint limits, the desired path cannot be successfully executed, as shown in Fig. 9 (dot dashed blue line). It can be observed that only in the first part of the commanded trajectory, before the joint limits occurrence, the path of the needle's tip has a circular shape; when the joint limits occur, the corresponding joint variables saturate and the actual path significantly deviates from the desired circular path. The desired circular trajectory, extrapolated using the part of the real trajectory not influenced by joint saturations, is depicted using dotted black line. This trajectory was commanded in simulation to the PSM arm with our MT. Since now the system is redundant, infinite solutions exist for the inverse kinematics problem and the redundancy could be used to efficiently avoid joint limits. In our problem, we do not explicitly exploit the redundancy; instead, we just want to show that a feasible solution could be easily found by a surgeon teleoperating the instrument. Therefore a simple solution corresponding to the minimum norm velocity is computed by using the Jacobian pseudo-inverse; despite this, the joint limits are not violated and the desired path for the needle is respected as shown in Fig. 9 (red continuous line).

Quantitative results of the experiment are shown in Fig. 10. In particular, the figure shows the time histories of the joint variables $\boldsymbol{q}$ using both the ST and the MT where the dashed lines represent the time history of the seventh joint, active only in the MT, and the dot-and-dash lines represent the time history of the sixth joint, which reaches its upper limit in the ST. It is clear that, with our MT, the redundancy allows to avoid the joint limits. This is quantitatively explained by considering the weighted dexterity index, better described in the Appendix, which allows evaluating the manipulator's overall ability to move, by tacking into account the distance from both joint limits and singularities. This index has been chosen because it allows comparing the dexterity of manipulators with the same task space dimension independently from the joint space dimension, thus it constitutes a suitable measure of the introduced enhancements. As it can be seen from Fig. 10, this measure remains greater than zero for the whole trajectory execution only when the MT is used.

TABLE IV
SUTURE PROCEDURES

	Expertise	Type	Needle	Joint limit
SU1	Novice	Planar vertical	GL-222	NO
SU2	Novice	Planar 15°	GL-222	YES
SU3	Novice	Planar 20°	RB-1	YES
SU4	Novice	Planar 110°	RB-1	NO
SU5	Novice	Planar 20°	RB-1	YES
SU6	Intermediate	Planar vertical	UR-6	NO
SU7	Intermediate	Planar vertical	UR-6	NO
SU8	Intermediate	Planar vertical	UR-6	NO
SU9	Intermediate	Planar vertical	UR-6	NO
SU10	Intermediate	Planar vertical	UR-6	NO
SU11	Expert	Circular vessel	UR-6	NO
SU12	Expert	Circular vessel	UR-6	NO
SU13	Expert	Circular vessel	UR-6	YES

TABLE V
OVERALL PERFORMANCE OF THE MT

	Stitches	Reorient	Help	Success
#	65	45	30	25
		Reorient/Stitches	Help/Reorient	Success/Reorient
%		69%	66%	55%

C. *Second Case Study: Complete Suturing Procedures*

In the second case study, the set of suturing procedures reported in Table IV was recorded. The sutures have been executed by novice (N), intermediate (I) and expert (E) surgeons, using three types of needles. The procedures consist in 10 planar sutures with different wound angles, executed on two different types of phantoms, and 3 circular anastomosis on a vessel phantom. Each suture consists of 5 stitches. In the table, for each suture, it is also indicated if a joint limit was reached at least once.

The 13 suturing procedures have been monitored and, for each sequence of 5 stitches, the following data have been evaluated and reported in Fig. 11 (Top):

- the number of stitches that required needle reorientation (gray bars);
- the number of reorientations performed along the needle tangent, for which the MT would have been helpful (red bars);
- the number of reorientations with rotation angles that were lower than the maximum rolling angles for the used needle (considering the values reported in Table I), for which the MT would have been successful (blue bars).

The overall performance is summarized in Table V. It can be seen that 69% of the stitches required reorientation and that the MT would be helpful in the 66% of the situations, allowing to complete the reorientation in the 55% of the cases.

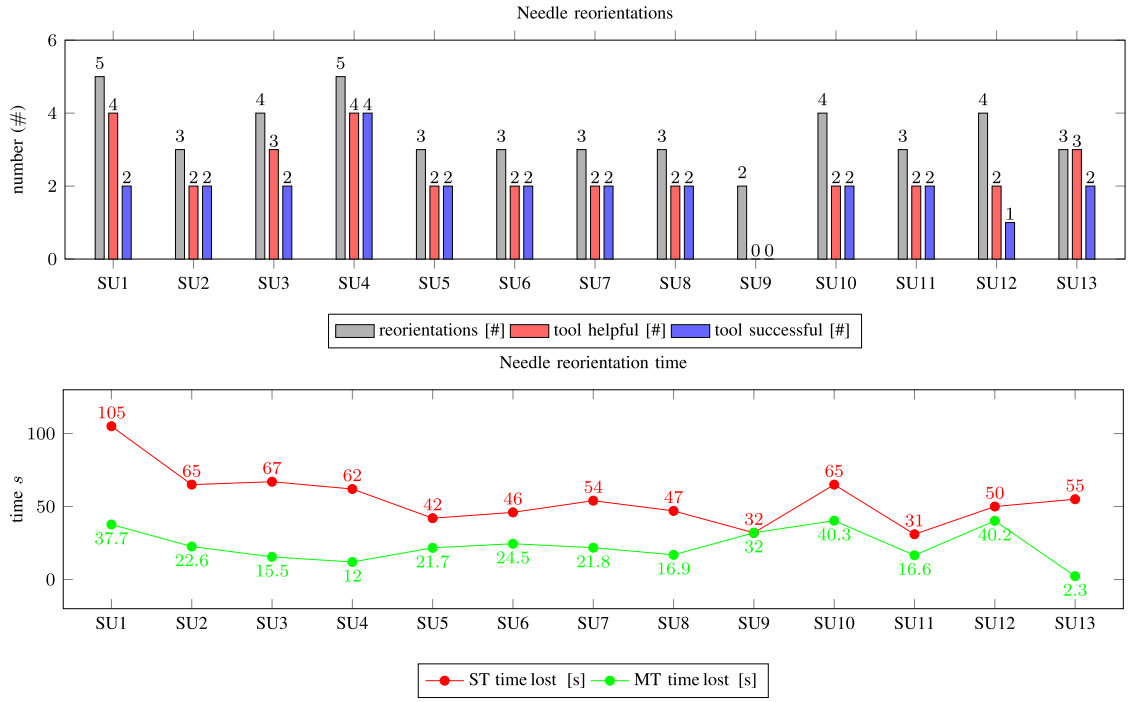

Fig. 11. Collected data in 13 sutures (SU1, . . . , SU13) composed of 5 stitches. Top: Number of stitches requiring needle reorientation for each suture (gray bar), number of reorientations for which the MT would have been helpful (red bar), number of reorientations for which the MT would have been successful (blue bar). Bottom: Total time lost for reorienting the needle with the ST (red line) and with the MT (green line).

To get a better understanding of the problems encountered during the suture performance we asked the surgeons to explain the reasons of each reorientation. In the 37.1% of the cases we found that the needle was dropped to move organs or to make knots and wasn't in the optimal orientation; in the 48.6% of the cases the needle was gripped in a bad orientation; finally, in the 14.3% of the cases, the needle lost the correct orientation during the stitch execution and needed to be reoriented.

Furthermore, for each suturing procedure, the total time lost in reorienting the needle was recorded. The results are reported in Fig. 11 (Bottom, red line). This time can be compared to the predicted reorientation time using the MT, reported in the same plot (green line). This latter has been computed as follows:

- for the reorientations that can be performed with the MT (i.e., those classified as successful and represented by the blue bars in Fig. 11), the execution time have been estimated considering a velocity of about 45 deg/sec for the rolling degree of freedom of the tool;
- for all the other reorientations the same time measured during he execution of the real stitch with a standard tool has been considered.

The results show that the MT allows a significant reduction of the time spent for needle reorientation.

VI. Conclusions and Future Works

In this work, a new concept of robotic surgical tool designed for in-hand manipulation of a suturing needle is shown. The mechanical design has been validated through a 2:1 scale prototype. Moreover, a comparison between real suturing procedures, using a standard tool, and simulated procedures, using the proposed modified tool, has been presented. The results show that the robot's dexterity improves when the modified tool is used. Moreover, the in-hand needle reorientation capability of the modified tool allows a significant reduction of the execution time of complete suturing procedures. In future works, a real prototype of the proposed tool with standard dimensions will be realized using materials suitable for sterilization and for real surgical interventions. Moreover, the tool functionalities will be evaluated in both ex vivo and in vivo procedures performed by a statistically significant population of both novice and expert surgeons. For this purpose, a device integrated in the dVRK robot master device will be designed to allow precise and real-time control of the new advanced tool. Suitable shared control algorithms will be adopted to exploit the redundancy introduced by our novel tool in order to cope with the joints limits and to maximize the dexterity. Finally, a study will be done to evaluate the best needle surface and material to maximize gripping and rolling capabilities.

Appendix

In order to quantitatively evaluate the benefits introduced by our tool, a dexterity analysis has been performed along suturing trajectories. A suitable dexterity measure has been used to quantify the overall motion capability of the robot with the new tool in comparison with the same robot using a standard da Vinci tool. This measure can be computed directly starting from the robot Jacobian matrix.

The influence of the joint limits on the robot's dexterity can be taken into account by weighting the entries of the

Jacobian matrix according to a joint limits performance criterion as in [20]. More in detail, a penalization matrix $L(\boldsymbol{q}) \in \mathbb{R}^{r\times n}$ is introduced, where r and n are the task and the joint space dimensions, respectively. This matrix is used to compute the elements of the augmented Jacobian $\tilde{J}(\boldsymbol{q}) \in \mathbb{R}^{r\times n}$ as

$$\tilde{J}_{i,j}(\boldsymbol{q}) = L_{i,j}(\boldsymbol{q}) J_{i,j}(\boldsymbol{q}), \quad i = 1,\dots r, \quad i = 1,\dots n, \quad (5)$$

where $J_{i,j}(\boldsymbol{q})$ is the (i,j) element of the robot Jacobian and $L_{i,j}(\boldsymbol{q})$ is defined as

$$L_{i,j}(\boldsymbol{q}) = \frac{1}{\sqrt{1+|\nabla h_j(\boldsymbol{q})|}}. \quad (6)$$

The scalar function $h(\boldsymbol{q}) : \mathbb{R}^n \to \mathbb{R}$ in (6) is a differentiable function of the joint vector $\boldsymbol{q}$ which tends to infinity as the joint variables approach the corresponding joint limits. In this work, taking inspiration from [21], we use the following function

$$h(\boldsymbol{q}) = \sum_{i=1}^{n} \frac{1}{4} \frac{(q_{i,\max} - q_{i,\min})^2}{(q_{i,\max} - q_i)(q_i - q_{i,\min})}. \quad (7)$$

The gradient $\nabla h(\boldsymbol{q})$ represents the direction of fastest increase of $h(\boldsymbol{q})$ and is useful to build the corresponding penalization index (6). The i-th component of the gradient $\nabla h_i(\boldsymbol{q}) = \partial h(\boldsymbol{q})/\partial q_i$ can be computed as

$$\nabla h_i(\boldsymbol{q}) = \frac{1}{4} \frac{(q_{i,\max} - q_{i,\min})^2 (2q_i - q_{i,\max} - q_{i,\min})}{(q_{i,\max} - q_i)^2 (q_i - q_{i,\min})^2}. \quad (8)$$

At this point, according to [22], a weighted dexterity measure d can be computed from the augmented Jacobian as:

$$d = \frac{\sqrt{rn}}{\sqrt{\mathrm{tr}\left[\left(\tilde{J}\tilde{J}^{\mathrm{T}}\right)^{-1}\right]}}, \quad (9)$$

where $\mathrm{tr}(\cdot)$ denote the trace operator. This index provides similar information of the standard manipulability index, but allows comparing manipulators with the same task space dimension independently from the joint space dimension. Moreover, it takes into account the distance from both joint limits and singularities.

REFERENCES

[1] P. Francis *et al.*, "Miniaturized instruments for the da Vinci research kit: Design and implementation of custom continuum tools," *IEEE Robot. Autom. Mag.*, vol. 24, no. 2, pp. 24–33, Jun. 2017.

[2] D. Martin, J. Woodard, C. Shurtleff, and A. Yoo, "Articulating needle driver," U.S. Patent 13/466,188, Nov. 15, 2012.

[3] S. Sen, A. Garg, D. V. Gealy, S. McKinley, Y. Jen, and K. Goldberg, "Automating multi-throw multilateral surgical suturing with a mechanical needle guide and sequential convex optimization," *IEEE Int. Conf. Robot. Autom.*, 2016, pp. 4178–4185.

[4] M. Selvaggio, S. Grazioso, G. Notomista, and F. Chen, "Towards a self-collision aware teleoperation framework for compound robots," in *Proc. IEEE World Haptics Conf.*, Jun. 2017, pp. 460–465.

[5] M. Selvaggio, G. Notomista, F. Chen, B. Gao, F. Trapani, and D. Caldwell, "Enhancing bilateral teleoperation using camera-based online virtual fixtures generation," in *Proc. IEEE/RSJ Int. Conf. Intell. Robots Syst.*, 2016, pp. 1483–1488.

[6] A. Spiers, S. Baillie, T. Pipe, and R. Persad, "Experimentally driven design of a palpating gripper with minimally invasive surgery considerations," in *Proc. IEEE Haptics Symp.*, 2012, pp. 261–266.

[7] N. Rahman, L. Carbonari, M. D'Imperio, C. Canali, D. G. Caldwell, and F. Cannella, "A dexterous gripper for in-hand manipulation," in *Proc. IEEE Int. Conf. Adv. Intell. Mechatronics*, Jul. 2016, pp. 377–382.

[8] N. Rahman *et al.*, "A novel bio-inspired modular gripper for in-hand manipulation," in *Proc. IEEE Int. Conf. Robot. Biomimetics*, Dec. 2015, pp. 7–12.

[9] N. Rojas, R. R. Ma, and A. M. Dollar, "The GR2 gripper: An underactuated hand for open-loop in-hand planar manipulation," *IEEE Trans. Robot.*, vol. 32, no. 3, pp. 763–770, Jun. 2016.

[10] R. M. Greenhalgh, "Techniques of anastomosis," in *Vascular Surgical Techniques.* Oxford, U.K.: Butterworth-Heinemann, 1984, pp. 5–13.

[11] F. Fazioli, F. Ficuciello, G. A. Fontanelli, B. Siciliano, and L. Villani, "Implementation of a soft-rigid collision detection algorithm in an open-source engine for surgical realistic simulation," in *Proc. IEEE Int. Conf. Robot. Biomimetics*, 2016, pp. 2204–2208.

[12] A. Talasaz, A. L. Trejos, and R. V. Patel, "The role of direct and visual force feedback in suturing using a 7-DOF dual-arm teleoperated system," *IEEE Trans. Haptics*, vol. 10, no. 2, pp. 276–287, Apr.–Jun. 2017.

[13] G. A. Fontanelli, L. Buonocore, F. Ficuciello, L. Villani, and B. Siciliano, "A novel force sensing integrated into the trocar for minimally invasive robotic surgery," in *Proc. IEEE/RSJ Int. Conf. Intell. Robots Syst.*, 2017, pp. 131–136.

[14] A. Petit, F. Ficuciello, G. A. Fontanelli, L. Villani, and B. Siciliano, "Using physical modeling and RGB-D registration for contact force sensing on deformable objects," in *Proc. IEEE Int. Conf. Informat. Control, Autom. Robot.*, 2017, pp. 24–33.

[15] N. Ahmidi *et al.*, "A dataset and benchmarks for segmentation and recognition of gestures in robotic surgery," *IEEE Trans. Biomed. Eng.*, vol. 64, no. 9, pp. 2025–2041, Sep. 2017.

[16] P. Kazanzides *et al.*, "An open-source research kit for the da Vinci surgical system," in *Proc. IEEE Int. Conf. Robot. Autom.*, May 2014, pp. 6434–6439.

[17] T. Ahlering, *Da Vinci Prostatectomy 3-Arm and 4-Arm Approach*. Sunnyvale, CA, USA: Intuitive Surgical, Inc., 2013.

[18] G. A. Fontanelli, F. Ficuciello, L. Villani, and B. Siciliano, "Modelling and identification of the da Vinci research kit robotic arms," in *Proc. IEEE/RSJ Int. Conf. Intell. Robots Syst.*, 2017, pp. 1464–1469.

[19] B. Siciliano, L. Sciavicco, L. Villani, and G. Oriolo, *Robotics: Modelling, Planning and Control*. Berlin, Germany: Springer, 2010.

[20] N. Vahrenkamp, T. Asfour, G. Metta, G. Sandini, and R. Dillmann, "Manipulability analysis," in *Proc. IEEE-RAS Int. Conf. Hum. Robots*, 2012, pp. 568–573.

[21] T. F. Chan and R. V. Dubey, "A weighted least-norm solution based scheme for avoiding joint limits for redundant joint manipulators," *IEEE Trans. Robot. Autom.*, vol. 11, no. 2, pp. 286–292, Apr. 1995.

[22] S. Tadokoro, I. Kimura, and T. Takamori, "A dexterity measure for trajectory planning and kinematic design of redundant manipulators," in *Proc. Annu. Conf. IEEE Ind. Electron. Soc.*, 1989, pp. 415–420.